CORRELATION BETWEEN MULTIPARTICLE CUMULANTS AND MEAN TRANSVERSE MOMENTUM IN SMALL COLLISION SYSTEMS WITH THE CMS DETECTOR*

Shengquan Tuo

for the CMS Collaboration

Vanderbilt University, Nashville, TN, USA

Received 23 August 2022, accepted 7 October 2022, published online 14 December 2022

Correlations between multiparticle cumulants and mean transverse momentum in proton–proton (pp), proton–lead (pPb), and peripheral lead–lead (PbPb) collisions are presented as a function of charged-particle multiplicity. The data, corresponding to integrated luminosities of 28.6 pb^{-1} for pp at $\sqrt{s} = 13$ TeV, 186 nb^{-1} for pPb at $\sqrt{s_{_{NN}}} = 8.16$ TeV, and 0.58 nb^{-1} for PbPb at $\sqrt{s_{_{NN}}} = 5.02$ TeV, were collected using the CMS detector at the LHC. The two- and four-particle cumulants for the second- and third-order Fourier harmonics are correlated with the mean transverse momentum on an event-by-event basis. Sign changes are observed when using two-particle cumulants in pp and pPb systems. No sign change is observed as pseudorapidity gaps between the two subevents increase. Predictions based on color-glass condensate and hydrodynamic models are compared to the experimental results.

DOI:10.5506/APhysPolBSupp.16.1-A67

1. Introduction

A hot and dense medium known as the quark–gluon plasma (QGP) has been extensively studied using heavy-ion collisions at the Relativistic Heavy-Ion Collider and the Large Hadron Collider [1]. The azimuthal anisotropy of the produced particles in these collisions is a powerful tool to study the collective dynamics and transport properties of the QGP [2]. This anisotropy is characterized by the Fourier coefficients (v_n) of the particle azimuthal angle (ϕ) distribution $\mathrm{d}N/\mathrm{d}\phi \propto 1 + 2\sum_n v_n \cos[n(\phi - \Psi_n)]$, where v_n and Ψ_n represent the amplitude and phase of the n^{th}-order azimuthal flow vector [3].

* Presented at the 29$^{\mathrm{th}}$ International Conference on Ultrarelativistic Nucleus–Nucleus Collisions: Quark Matter 2022, Kraków, Poland, 4–10 April, 2022.

In a hydrodynamic picture, the Fourier harmonics are the result of final-state effects since they come from the final-state response to the initial geometry of the colliding system [4]. In the past decade, a remarkable similarity in the azimuthal anisotropy signatures has been observed between heavy-ion collisions and smaller collision systems, such as proton–proton (pp), proton–lead (pPb), and peripheral lead–lead (PbPb) [5]. The similarity holds even for multiparticle correlations, which can suppress "nonflow" effects from few particle correlations. The observed anisotropy in small systems can originate from the final-state response to the initial geometry, as well as from initial-state effects as described by the color-glass condensate effective theory [6]. The dominant origin of the azimuthal anisotropy in small systems is still under active discussion [1, 5] because there is not a clear observable that can distinguish the final-state effects from the initial-state effects.

In addition to generating final-state azimuthal anisotropy from initial spatial anisotropy, hydrodynamic response to the overall size of the initial overlapping area of the two colliding particles results in radial flow, which is reflected by the mean transverse momentum $[p_{\mathrm{T}}]$ on an event-by-event basis. The correlations between radial and anisotropic flow can be quantified using a modified Pearson correlator [7]

$$\rho\left(v_n^2, [p_{\mathrm{T}}]\right) = \frac{\mathrm{cov}\left(v_n^2, [p_{\mathrm{T}}]\right)}{\sqrt{\mathrm{Var}\left(v_n^2\right)_{\mathrm{dyn}}}\sqrt{\mathrm{Var}\left([p_{\mathrm{T}}]\right)_{\mathrm{dyn}}}}\,, \tag{1}$$

where $\mathrm{cov}(v_n^2, [p_{\mathrm{T}}])$ is the covariance between v_n^2 and $[p_{\mathrm{T}}]$, and $\mathrm{Var}(v_n^2)_{\mathrm{dyn}}$ and $\mathrm{Var}([p_{\mathrm{T}}])_{\mathrm{dyn}}$ are the dynamical variances of the v_n^2 and $[p_{\mathrm{T}}]$ distributions, respectively. The dynamical variances remove the autocorrelation effects when compared to variances of v_n^2 and $[p_{\mathrm{T}}]$ distributions. It was found that this correlator is sensitive to the degree of subnucleon fluctuations, and its strength can be traced back to the initial density profile [8].

Recently, it was suggested that this correlator might be able to distinguish between initial- and final-state effects [9]. A characteristic sign change of the modified Pearson correlator as a function of charged particle multiplicity is predicted in small collision systems. No sign change is present without the initial-state effects suggested by color-glass condensate effective theory. However, it was found that in PYTHIA 8, a sign change exists due to nonflow effects [10, 11]. Measurements of the correlator with proper treatment of nonflow effects, and corresponding searches for correlator sign changes in low multiplicity pp, pPb, and peripheral PbPb collisions can provide insights into the origin of the azimuthal correlations in small systems.

In these proceedings, the correlators are measured for the first time using four-particle cumulants instead of two-particle correlation techniques in pp, pPb, and peripheral PbPb collisions. Nonflow effects are further studied using different pseudorapdity (η) gap sizes. In addition, the correlators for the third Fourier harmonic are presented for the first time in the three small collision systems as a function of charged-particle multiplicity.

2. Multiparticle cumulants and mean transverse momentum correlations

All previous studies of the correlator use v_n^2 from two-particle correlations in Eq. (1). The v_n^2 term can be rewritten as the two-particle cumulant since $c_n\{2\} = \left\langle e^{in(\phi_1-\phi_2)} \right\rangle = v_n\{2\}^2$ [12]. To remove nonflow in the two-particle v_n, all previous measurements applied the subevent method which introduces subevents that are separated in different η ranges [13, 14]. With two subevents for $c_n\{2\}$, the covariance of the correlator in Eq. (1) is

$$\mathrm{cov}(c_n\{2\}, [p_{\mathrm{T}}]) = \mathfrak{Re}\left\langle \sum_{a,b} \exp^{in(\phi_a-\phi_b)} \left([p_{\mathrm{T}}] - \langle [p_{\mathrm{T}}] \rangle\right) \right\rangle , \tag{2}$$

where ϕ_a and ϕ_b are the azimuthal angles of particles a and b in subevents A and B, respectively. The $\langle [p_{\mathrm{T}}] \rangle$ is the average $[p_{\mathrm{T}}]$ in all the events at a certain multiplicity range. We select tracks with $\eta < -0.75$ to be subevent A, while tracks with $\eta > 0.75$ belong to subevent B. Tracks in the middle region $|\eta| < 0.5$ are used to obtain $[p_{\mathrm{T}}]$ in each event. The selections make sure subevents A and B are symmetric in η, and that there is a minimum η gap of 1.5 between them to reduce nonflow effects.

The remaining nonflow problem is addressed with two approaches. In the first approach, we increase the minimum η gap between subevents A and B from 1.5 to 2.0, by changing $c_2\{2\}$ analysis using particles in $|\eta| > 0.75$ to $|\eta| > 1.0$. In the second approach, we extend the current observable by replacing $c_2\{2\}$ with four-particle cumulant $c_2\{4\}$ [15]. Particles in $|\eta| > 0.75$ are divided into three equal η regions to obtain $c_2\{4\}$ in each event. The event-by-event $c_2\{4\}$ is then correlated with $[p_{\mathrm{T}}]$ in the same event. The results are presented as a function of tracking efficiency corrected multiplicity N_{ch} using particles within $0.5 < p_{\mathrm{T}} < 5$ GeV and $|\eta| < 2.4$. Details about the CMS detector and this analysis can be found in [15, 16].

3. Results for the covariances and correlators

The measurements of covariances from two- and four-particle correlations for harmonics $n = 2$ and $n = 3$ in 13 TeV *pp*, 8.16 TeV *p*Pb, and 5.02 TeV PbPb collisions are presented in Fig. 1. In both *pp* and *p*Pb collisions, $\mathrm{cov}(c_2\{2\}, [p_{\mathrm{T}}])$ has a sign change from positive to negative as N_{ch} increases. The results are consistent with the prediction of a sign change feature from the color-glass condensate model. To compare $\mathrm{cov}(c_2\{2\}, [p_{\mathrm{T}}])$

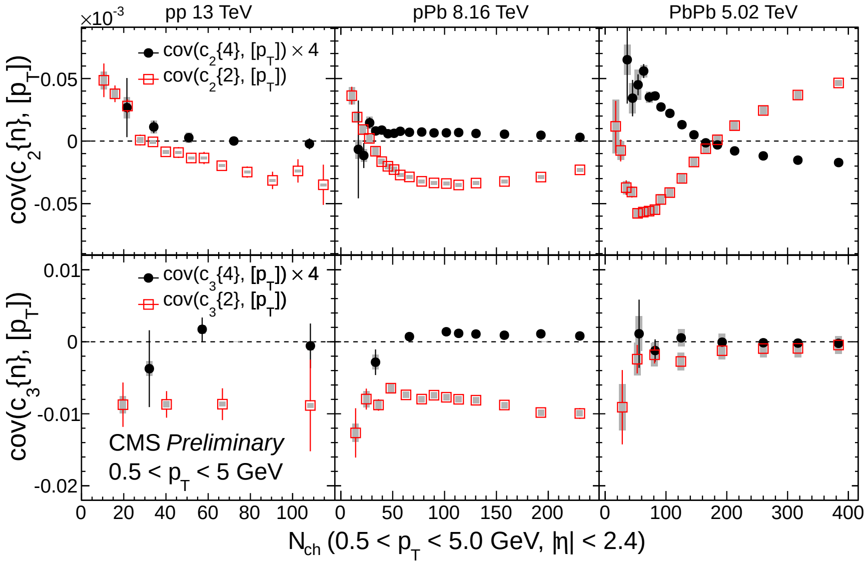

Fig. 1. The covariances of cumulants from two- and four-particle correlations and $[p_{\mathrm{T}}]$ as a function of N_{ch} in 13 TeV pp (left), 8.16 TeV pPb (middle), and 5.02 TeV PbPb (right). The top (bottom) panels are for harmonic $n = 2$ ($n = 3$). The error bars correspond to statistical uncertainties, while the shaded areas denote the systematic uncertainties. The figure is taken from Ref. [15].

and $\mathrm{cov}(c_2\{4\}, [p_{\mathrm{T}}])$ on the same scale, the values of $\mathrm{cov}(c_2\{4\}, [p_{\mathrm{T}}])$ are multiplied by 4 in all the panels. No clear sign change is observed for $\mathrm{cov}(c_2\{4\}, [p_{\mathrm{T}}])$ in both pp and pPb with the current statistical precision. As N_{ch} decreases in PbPb, the values of $\mathrm{cov}(c_2\{2\}, [p_{\mathrm{T}}])$ change from positive to negative, reach a minimum at $N_{\mathrm{ch}} = 60$, and then approach zero at the lowest N_{ch} range.

The correlator with a larger η range ($|\eta| > 1.0$) for the cumulant is shown in Fig. 2. In both pp and pPb collisions, the sign change at low N_{ch} disappears with the larger η gap between the two subevents, which is similar to calculations using PYTHIA 8 [17]. The predictions in pPb collisions at 5.02 TeV from the IP-Glasma+MUSIC+UrQMD model [9] with $0.5 < p_{\mathrm{T}} <$ 5 GeV are compared to the data. This model includes gluon saturation in the initial-state followed by hydrodynamic evolution and hadronic interactions. The characteristic sign change of the correlator predicted by this model is observed at the same N_{ch} location for $|\eta| > 0.75$, but it disappears when using $|\eta| > 1.0$, which leads to less nonflow. The results indicate that after removing more nonflow, the color-glass condensate signal is not observed.

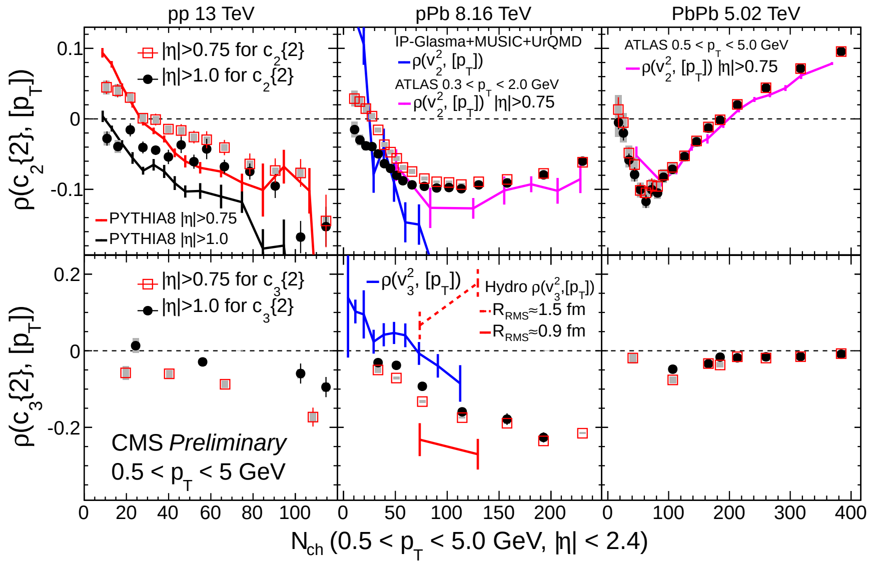

Fig. 2. (Color online) The correlator using two-particle cumulant from $|\eta| > 0.75$ and $|\eta| > 1.0$ as a function of N_{ch} in 13 TeV pp (left), 8.16 TeV pPb (middle), and 5.02 TeV PbPb (right). The top (bottom) panels are for harmonic $n = 2$ ($n = 3$). The error bars correspond to statistical uncertainties, while the shaded areas denote the systematic uncertainties. Calculations from PYTHIA 8 (left higher/red and lower/black lines), and IP-Glasma+MUSIC+UrQMD (middle black/blue lines) [9] are compared to the data. The figure is taken from Ref. [15].

4. Summary

In summary, apparent sign changes in the modified Pearson correlators are observed as a function of charged-particle multiplicity when using two-particle cumulants with $|\eta| > 0.75$, making the minimum η gap of 1.5, in pp and pPb systems. The sign changes disappear when the nonflow is suppressed using $|\eta| > 1.0$, making the minimum η gap of 2.0. The correlations of four-particle cumulants $c_2\{4\}$ with the mean p_{T} show no sign change, similar to the two-particle correlation results with a larger η gap. These high-precision data and the observables employing multiparticle correlators shown here provide new insight into the origin of azimuthal anisotropy in small collision systems.

REFERENCES

[1] W. Busza, K. Rajagopal, W. van der Schee, *Annu. Rev. Nucl. Part. Sci.* **68**, 339 (2018).

[2] U. Heinz, R. Snellings, *Annu. Rev. Nucl. Part. Sci.* **63**, 123 (2013).

[3] A.M. Poskanzer, S.A. Voloshin, *Phys. Rev. C* **58**, 1671 (1998).

[4] B.H. Alver, C. Gombeaud, M. Luzum, J.-Y. Ollitrault, *Phys. Rev. C* **82**, 034913 (2010).

[5] J.L. Nagle, W.A. Zajc, *Annu. Rev. Nucl. Part. Sci.* **68**, 211 (2018).

[6] B. Schenke, S. Schlichting, R. Venugopalan, *Phys. Lett. B* **747**, 76 (2015).

[7] P. Bożek, *Phys. Rev. C* **93**, 044908 (2016).

[8] G. Giacalone, F.G. Gardim, J. Noronha-Hostler, J.-Y. Ollitrault, *Phys. Rev. C* **103**, 024909 (2021).

[9] G. Giacalone, B. Schenke, C. Shen, *Phys. Rev. Lett.* **125**, 192301 (2020).

[10] C. Zhang, A. Behera, S. Bhatta, J. Jia, *Phys. Lett. B* **822**, 136702 (2021).

[11] S.H. Lim, J.L. Nagle, *Phys. Rev. C* **103**, 064906 (2021).

[12] A. Bilandzic, R. Snellings, S. Voloshin, *Phys. Rev. C* **83**, 044913 (2011).

[13] ATLAS Collaboration (G. Aad *et al.*), *Eur. Phys. J. C* **79**, 985 (2019).

[14] ALICE Collaboration (S. Acharya *et al.*), *Phys. Lett. B* **834**, 137393 (2022).

[15] CMS Collaboration, CMS Physics Analysis Summary, CMS-PAS-HIN-21-012, 2022, `https://cds.cern.ch/record/2805932`

[16] S. Chatrchyan *et al.*, *J. Instrum.* **3**, S08004 (2008).

[17] T. Sjöstrand *et al.*, *Comput. Phys. Commun.* **191**, 159 (2015).